PROCEEDINGS OF SCIENCE

Limits on WIMP-Scattering Cross Sections using Solar Neutrinos with Ten Years of IceCube Data

The IceCube Collaboration

(a complete list of authors can be found at the end of the proceedings)

E-mail: jeffrey.lazar@uclouvain.be

Although dark matter (DM) comprises 84% of the matter content of the Universe, its nature remains unknown. One broad class of particle DM motivated by extensions of the Standard Model (SM) is weakly interacting massive particles (WIMPs). Generically, WIMPs will scatter off nuclei in large celestial bodies such as the Sun, thus becoming gravitationally bound. Subsequently, WIMPs can annihilate to stable SM particles, ultimately releasing most of their energy as high-energy neutrinos which escape from the Sun. Thus, an excess of neutrinos from the Sun's direction would be evidence for WIMPs. The IceCube Neutrino Observatory is well-suited to such searches since it is sensitive to WIMPs with masses in the region preferred by supersymmetric extensions of the SM. I will present the results of IceCube's most recent solar WIMP search, which includes all neutrino flavors, covers the WIMP mass range from 20 GeV to 10 TeV, and has world-leading sensitivity over this entire range for most channels considered.

Corresponding authors: Jeffrey Lazar[1*]

[1] *Université Catholique de Louvain, Pl. de l'Université 1, 1348 Ottignies-Louvain-la-Neuve*

[*] Presenter

39th International Cosmic Ray Conference (ICRC2025)
15–24 July 2025
Geneva, Switzerland

ICRC 2025
The Astroparticle Physics Conference
Geneva July 15-24, 2025

© Copyright owned by the author(s) under the terms of the Creative Commons Attribution-NonCommercial-NoDerivatives 4.0 International License (CC BY-NC-ND 4.0).

PoS(ICRC2025)502

1. Introduction

Dark matter (DM) makes up about 84% of all matter in the Universe [1] and may consist of fundamental particles [2]. A worldwide effort is underway to detect these particles [3–6], with particular interest in weakly interacting massive particles, which interact with Standard Model (SM) particles at or below the weak scale. If DM is comprised of such particles, they could scatter off nuclei in the Sun, lose energy, and become gravitationally trapped by its gravity [7]. Through continued interactions, DM would accumulate at the Sun's core. Eventually, these particles would annihilate into SM particles, but only neutrinos, due to their weak interactions, could escape the dense solar interior. This opens a pathway for indirect DM detection by observing an excess of high-energy neutrinos coming from the Sun. Because DM capture and annihilation rates in the Sun are expected to reach equilibrium [7], such neutrino-based searches are sensitive to the DM-proton scattering cross section. This approach complements direct detection methods on Earth, which look for energy from nuclear recoils caused by DM interactions [3].

The IceCube Neutrino Observatory, located near the geographic South Pole, is a gigaton-scale Cherenkov detector embedded in the Antarctic ice. It comprises 5,160 digital optical modules (DOMs) arranged along 86 vertical strings, each holding 60 modules. These DOMs detect Cherenkov light emitted by relativistic charged particles produced in neutrino interactions. The DOMs are spaced 17 m apart vertically in the main array on a hexagonal grid with 125 m between strings. The denser DeepCore sub-array features a tighter configuration, with 7 m vertical spacing and about 70 m spacing between strings. Together, the main array and DeepCore allow IceCube to detect neutrinos across a wide energy range, from 5 GeV to PeV. This capability enables IceCube to probe a dark matter mass range comparable to that of direct detection experiments.

2. Simulation and Data Sample

This analysis combines IceCube's low-energy event selection—initially developed for measuring atmospheric neutrino oscillation parameters [8]—with the high-energy selection used in searches for neutrino emission from astrophysical point sources [9]. The only modification to these selections is the addition of a filter to remove any overlap between the two selections, ensuring statistical independence. The high-energy selection targets a high-purity sample of charged-current ν_μ events. At energies above $\approx$ 300 GeV, the resulting $\mu^\pm$ can travel more than a kilometer [10], creating long, track-like signals that allow for precise directional reconstruction.

In contrast, the low-energy selection targets events in a regime where muons produce less light and travel shorter distances, reducing angular resolution. As a result, this sample includes neutrinos of all flavors rather than focusing on ν_μ alone.

Within the analysis energy range of 5 GeV to 10 TeV, the most common background comes from atmospheric neutrinos and muons produced by cosmic-ray interactions in Earth's atmosphere [11]. These backgrounds are modeled using real data, with reconstructed right ascension randomized for each event. This procedure is equivalent to time-scrambling the events in IceCube's local coordinate system. Since the Sun lies far from the equatorial poles, this scrambling diminishes any solar clustering, effectively removing point-source signatures while preserving the declination

PoS(ICRC2025)502

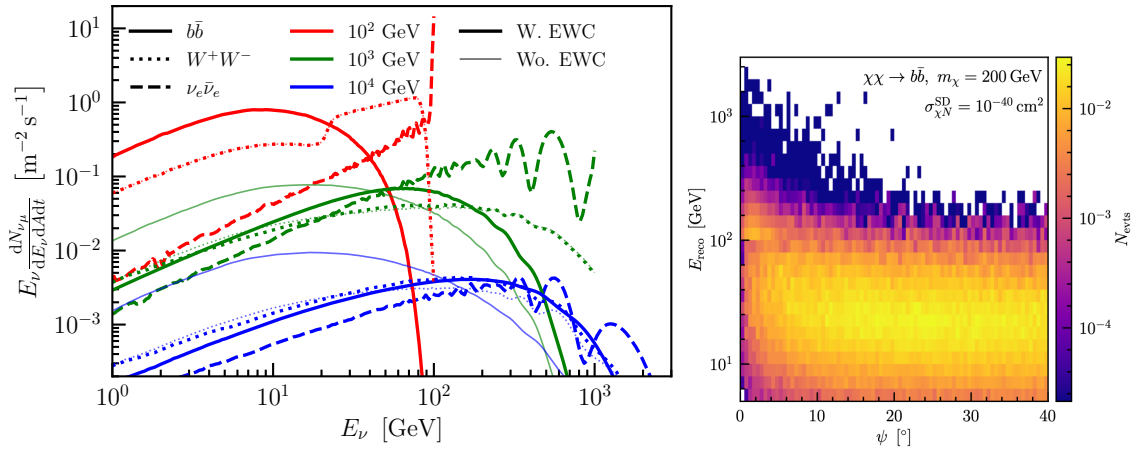


Figure 1: ***Spectra of neutrinos for several annihilation channels and WIMP masses at Earth and expected reconstructed event distribution.*** Left: The line styles represent a primary annihilation channel, while the colors represent different WIMP masses. Annihilation channels studied in previous IceCube analyses include a lower opacity line to show the spectra without the EW effect. Note the significant differences in the spectra from annihilation to $b\bar{b}$ at masses above the EW scale and the absence of such differences from annihilation to W^-W^+. Right: The expected distribution of events from 200 GeV DM annihilating to $b\bar{b}$ as a function of the reconstructed energy and reconstructed angular distance from the Sun.

dependence of background rates. This approach minimizes systematic uncertainties related to background modeling.

In addition to these backgrounds, this analysis also includes the background from solar atmospheric neutrinos, which are produced by cosmic-ray interactions within the solar atmosphere. To model this, this analysis adopts a recent model of the solar atmospheric neutrino flux [12], based on a hybrid solar density profile from Refs. [13–16] and computed using the `MCEq` cascade equation solver [17]. Neutrinos are generated from interactions of primary hadrons and secondary muons and are then propagated to Earth using the density matrix formalism implemented in the `nuSQuIDS` [18] package. The same framework handles the final propagation step from Earth's surface to the detector. The flux calculation also incorporates variations from cosmic-ray spectra and hadronic interaction models. For this analysis, we use the flux resulting from the combined Gaisser-Honda with Hillas-Gaisser H4a primary cosmic-ray flux [19] and Sibyll-2.3c hadronic interaction model [20, 21] assuming a purely protonic atmosphere and MRS prompt model [22].

To model the signal neutrinos from DM annihilation, this analysis employs the χ`aro`ν package [23]. This package assumes DM particles annihilate into a pair of monochromatic Standard Model particles. The spectra of resulting particles are drawn from precomputed tables, and all unstable particles are allowed to interact and decay until only neutrinos remain. This process uses a Monte Carlo method to model interactions and decays within the Sun's dense core. The resulting neutrino flux is then propagated to the detector using `nuSQuIDS`.

χ`aro`ν offers two approaches for generating the initial particle spectra: one using the PYTHIA 8.2 library [24] and another incorporating electroweak (EW) corrections [25]. EW effects become significant for DM masses above the EW scale, where decays may involve SM particles before electroweak symmetry breaking. While earlier models often neglected [26] or only approximated

PoS(ICRC2025)502

these effects [27], χaroν fully incorporates them. This effect can substantially alter the predicted neutrino spectra for specific annihilation channels. The left panel of Fig. 1 compares the propagated spectra with and without these effects for three DM masses and annihilation channels. At 100 GeV (below the EW scale), the spectra match across all channels. However, for 1 TeV and 10 TeV masses, a notable enhancement appears for the $b\bar{b}$ channel due to prompt weak boson emission producing hard neutrinos. In the W^-W^+ channel, the spectra shift slightly as energy is distributed across more weak bosons, leading to a softer neutrino output.

3. Analysis Methodology

For the analysis, data are binned based on reconstructed quantities to build expected distributions for background, solar atmospheric neutrinos, and neutrinos resulting from dark matter annihilation. In the high-energy selection, events are binned by reconstructed energy and their reconstructed angular separation from the Sun's center. An additional binning is applied for the low-energy selection using a morphological classification variable designed to distinguish charged-current ν_μ interactions from other event types. This variable is particularly useful because neutrinos originating from the Sun arrive in a flavor-mixed state, whereas atmospheric neutrinos above $\approx 40\,\text{GeV}$ tend to retain a ν_μ dominance. Consequently, detecting an excess of non-ν_μ events at specific energies can help differentiate a potential signal from the background.

Distributions for solar atmospheric neutrinos and DM-induced neutrinos are derived from Monte Carlo simulations. For each simulated event, a random time within the analysis window is selected, the Sun's position is calculated, and only events occurring within the Sun's physical extent are retained. This process is repeated numerous times, and the average is taken to find the expected time-averaged distributions.

In addition to modeling the solar atmospheric flux, simulations are performed for 51 dark matter scenarios, with DM masses ranging from 20 GeV and 10 TeV and annihilation into $b\bar{b}$, W^-W^+, $\tau^-\tau^+$, and $\nu_\alpha\bar{\nu}_\alpha$ channels. The right panel of Fig. 1 shows the predicted event rate for a benchmark DM model with a reference cross section of $\sigma_{\chi p} = 10^{-40}\,\text{cm}^2$ for both event selections. The low-energy distribution has been summed over the morphological discriminator for clarity in this figure. At energies above 100 GeV, the high-energy selection dominates, as indicated by event clustering within 3° of the Sun. At lower energies, where angular resolution decreases, events are distributed over a broader angular region. A slight discontinuity at 100 GeV reflects a selection cut applied to the reconstructed energy in the high-energy sample.

The data-derived background distribution is computed by taking all events that pass the selections and assigning a random right ascension drawn uniformly from the distribution $[0, 2\pi)$ and binning in the appropriate variables. Since there are typically not enough events to fill the bins with an appropriate sample size, this procedure is carried out tens of times, and the resulting distributions are averaged.

This analysis then uses a binned Poisson likelihood [28] given by:

$$\mathcal{L}(n|\theta) = \prod_i \frac{e^{-\mu_i(\theta)}\mu_i(\theta)^{n_i}}{n_i!},$$

PoS(ICRC2025)502

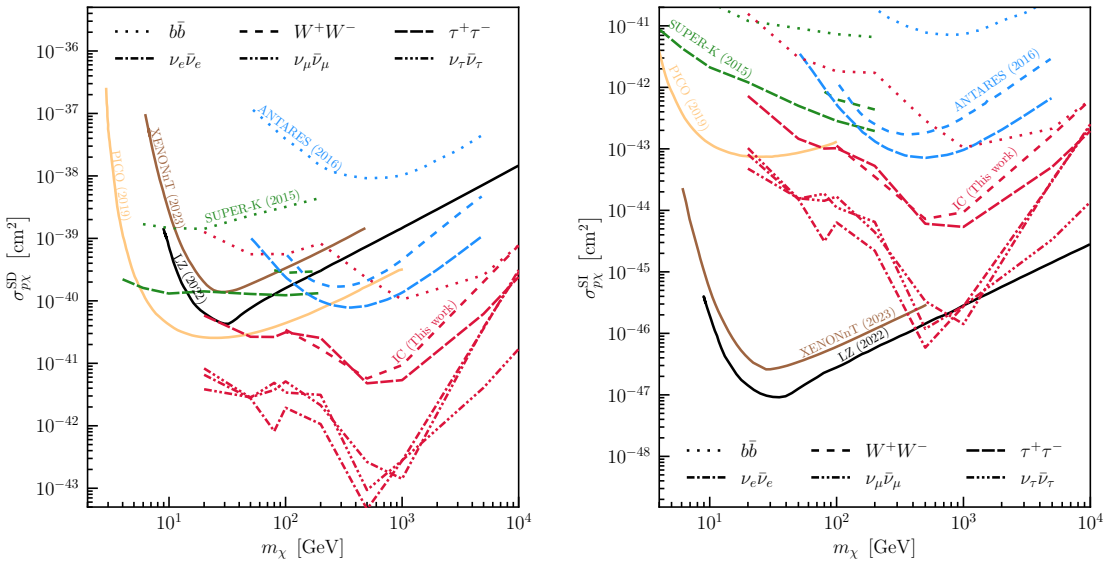


Figure 2: ***Limits on the spin-dependent and spin-independent DM-proton cross sections.*** Since no excess of neutrinos was observed from the direction of the Sun, limits on the spin-dependent WIMP-proton cross section are obtained. These new limits are compared to existing limits on this cross section from other experiments. Direct detection experiments are shown with solid lines, whereas indirect detection experiments are shown with linestyles corresponding to the annihilation channel. This analysis achieves world-leading limits for most annihilation channels for WIMPs above 100 GeV. Additionally, this analysis improves on the high-mass $b\bar{b}$ limits by more than an order of magnitude, highlighting the importance of the electroweak correction for hadronic annihilation channels. These limits are compared to the previous limits from PICO [29], ANTARES [30], XENONnT [31], LUX-ZEPLIN [32], and Super-Kamiokande [33].

where $\theta = (\alpha^\chi, \alpha^{\rm sa}, \alpha^{\rm a})$ is the model parameters, i.e. the DM, solar atmospheric, and conventional atmospheric normalizations relative to the nominal; $\mu(\theta)$ is the expected number of events in a particular model; n is the observed number of events; and i indexes the bin. To test the hypothesis, the test statistic is given by twice the log-likelihood ratio between the best fit with and without a contribution from DM:

$$\mathrm{TS} = -2\left[\log\left((n|\mathcal{L}(0,\,\hat{\alpha}^{\rm sa},\,\hat{\alpha}^{\rm a})\right) - \log\left(\mathcal{L}(n|\check{\alpha}^\chi,\,\check{\alpha}^{\rm sa},\,\check{\alpha}^{\rm a})\right)\right].$$

Here, $\hat{\alpha}^{\rm y}$ and $\check{\alpha}^{\rm y}$ denote the best-fit normalization in the background-only and signal-plus-background models, respectively. All background-only test-statistic distributions follow a modified χ^2 distribution with one degree of freedom, with the modifications arising from allowing only positive normalizations to be fit, leading to 50% of events having a test statistic of zero.

4. Results

Among the 51 dark matter (DM) scenarios examined in this analysis, 32 yielded best-fit results consistent with no DM contribution to the neutrino flux. Of the remaining 19 scenarios that favored a non-zero DM signal, only the case of 20 GeV DM annihilating into $b\bar{b}$ showed a preference for the DM-plus-Standard-Model hypothesis with a p-value below 0.1—specifically, a p-value of

PoS(ICRC2025)502

0.079, corresponding to a significance of 1.76σ. However, due to the low statistical significance and the large number of hypotheses tested, we do not claim evidence for a neutrino excess from DM annihilation in the Sun.

To set upper limits, we vary the DM contribution until the difference in the test statistic from the best-fit point reaches 1.64, corresponding to the 90% confidence level under the modified χ^2 distribution described earlier. The resulting constraints on spin-dependent and spin-independent DM-proton cross sections are shown in Fig. 2, alongside existing experimental bounds.

Several noteworthy features emerge from these limits. For DM annihilating to W^-W^+, $\tau^-\tau^+$, or $\nu_\alpha\bar{\nu}_\alpha$ pairs, this analysis probes previously unexplored regions of parameter space for DM masses above 100 GeV. Additionally, the limits on annihilation to $b\bar{b}$ at high DM masses are significantly improved, enhancing previous IceCube results by roughly a factor of 40, and surpassing ANTARES limits by about a factor of 100. Overall, this analysis sets the most stringent indirect detection limits for nearly all tested DM scenarios, with the sole exception being the 20 GeV $b\bar{b}$ case. These DM-proton cross section limits can also be reinterpreted as constraints on the DM-electron cross section. The leading global limits obtained from this analysis are presented in Fig. 3.

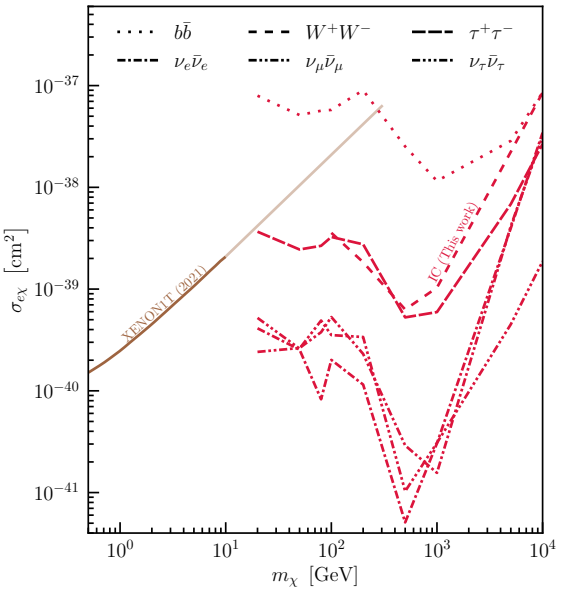


Figure 3: ***Limits on the DM-nucleon cross section.*** These new limits are compared to existing limits on this cross section from other experiments. Direct detection experiments are shown with solid lines, whereas indirect detection experiments are shown with linestyles corresponding to the annihilation channel. These limits are compared to results from the XENON1T [34]. Results scaled according to m_χ are shown as a lighter line for comparison at masses higher than had been reported in the original work.

References

[1] Katherine Freese. Status of Dark Matter in the Universe. *Int. J. Mod. Phys.*, 1(06):325–355, 2017.

[2] Gianfranco Bertone, Dan Hooper, and Joseph Silk. Particle dark matter: Evidence, candidates and constraints. *Phys. Rept.*, 405:279–390, 2005.

PoS(ICRC2025)502

[3] Jianglai Liu, Xun Chen, and Xiangdong Ji. Current status of direct dark matter detection experiments. *Nature Phys.*, 13(3):212–216, 2017.

[4] Jan Conrad and Olaf Reimer. Indirect dark matter searches in gamma and cosmic rays. *Nature Phys.*, 13(3):224–231, 2017.

[5] Oliver Buchmueller, Caterina Doglioni, and Lian Tao Wang. Search for dark matter at colliders. *Nature Phys.*, 13(3):217–223, 2017.

[6] Carlos A. Argüelles, Alejandro Diaz, Ali Kheirandish, Andrés Olivares-Del-Campo, Ibrahim Safa, and Aaron C. Vincent. Dark matter annihilation to neutrinos. *Rev. Mod. Phys.*, 93(3):035007, 2021.

[7] Gerard Jungman, Marc Kamionkowski, and Kim Griest. Supersymmetric dark matter. *Phys. Rept.*, 267:195–373, 1996.

[8] R. Abbasi et al. Measurement of Atmospheric Neutrino Oscillation Parameters Using Convolutional Neural Networks with 9.3 Years of Data in IceCube DeepCore. *Phys. Rev. Lett.*, 134(9):091801, 2025.

[9] R. Abbasi et al. Evidence for neutrino emission from the nearby active galaxy NGC 1068. *Science*, 378(6619):538–543, 2022.

[10] J. H. Koehne, K. Frantzen, M. Schmitz, T. Fuchs, W. Rhode, D. Chirkin, and J. Becker Tjus. PROPOSAL: A tool for propagation of charged leptons. *Comput. Phys. Commun.*, 184:2070–2090, 2013.

[11] T. K. Gaisser and M. Honda. Flux of atmospheric neutrinos. *Ann. Rev. Nucl. Part. Sci.*, 52:153–199, 2002.

[12] C. A. Argüelles, G. de Wasseige, A. Fedynitch, and B. J. P. Jones. Solar Atmospheric Neutrinos and the Sensitivity Floor for Solar Dark Matter Annihilation Searches. *JCAP*, 07:024, 2017.

[13] Hendrik C. Spruit. A model of the solar convection zone. *Sol Phys*, 34:277–290, 1974.

[14] John N. Bahcall, Aldo M. Serenelli, and Sarbani Basu. New solar opacities, abundances, helioseismology, and neutrino fluxes. *Astrophys. J. Lett.*, 621:L85–L88, 2005.

[15] J. M. Fontenla. Semiempirical Models of the Solar Atmosphere. II. The Quiet-Sun Low Chromosphere at Moderate Resolution. *Astrophys. J.*, 667:1243, 2007.

[16] O. Gingerich, R.W. Noyes, W. Kalkofen, and Y. Cuny. The Harvard-Smithsonian reference atmosphere. *Sol Phys*, 18:347–365, 1971.

[17] Anatoli Fedynitch, Ralph Engel, Thomas K. Gaisser, Felix Riehn, and Todor Stanev. Calculation of conventional and prompt lepton fluxes at very high energy. *EPJ Web Conf.*, 99:08001, 2015.

[18] Carlos A. Argüelles, Jordi Salvado, and Christopher N. Weaver. nuSQuIDS: A toolbox for neutrino propagation. *Comput. Phys. Commun.*, 277:108346, 2022.

[19] Anatoli Fedynitch, Julia Becker Tjus, and Paolo Desiati. Influence of hadronic interaction models and the cosmic ray spectrum on the high energy atmospheric muon and neutrino flux. *Physical Review D*, 86(11), December 2012.

[20] Felix Riehn, Ralph Engel, Anatoli Fedynitch, Thomas K. Gaisser, and Todor Stanev. Charm production in SIBYLL. *EPJ Web Conf.*, 99:12001, 2015.

[21] Felix Riehn, Ralph Engel, Anatoli Fedynitch, Thomas K. Gaisser, and Todor Stanev. A new version of the event generator Sibyll. *PoS*, ICRC2015:558, 2016.

PoS(ICRC2025)502

[22] A. D. Martin, M. G. Ryskin, and A. M. Stasto. Prompt neutrinos from atmospheric $c\bar{c}$ and $b\bar{b}$ production and the gluon at very small x. *Acta Phys. Polon. B*, 34:3273–3304, 2003.

[23] Qinrui Liu, Jeffrey Lazar, Carlos A. Argüelles, and Ali Kheirandish. χaroν: a tool for neutrino flux generation from WIMPs. *JCAP*, 10:043, 2020.

[24] Torbjörn Sjöstrand, Stefan Ask, Jesper R. Christiansen, Richard Corke, Nishita Desai, Philip Ilten, Stephen Mrenna, Stefan Prestel, Christine O. Rasmussen, and Peter Z. Skands. An Introduction to PYTHIA 8.2. *Comput. Phys. Commun.*, 191:159–177, 2015.

[25] Christian W. Bauer, Nicholas L. Rodd, and Bryan R. Webber. Dark matter spectra from the electroweak to the Planck scale. *JHEP*, 06:121, 2021.

[26] Carl Niblaeus, Ankit Beniwal, and Joakim Edsjo. Neutrinos and gamma rays from long-lived mediator decays in the Sun. *JCAP*, 11:011, 2019.

[27] Marco Cirelli, Gennaro Corcella, Andi Hektor, Gert Hutsi, Mario Kadastik, Paolo Panci, Martti Raidal, Filippo Sala, and Alessandro Strumia. PPPC 4 DM ID: A Poor Particle Physicist Cookbook for Dark Matter Indirect Detection. *JCAP*, 03:051, 2011. [Erratum: JCAP 10, E01 (2012)].

[28] S. Navas et al. Review of particle physics. *Phys. Rev. D*, 110(3):030001, 2024.

[29] C. Amole et al. Dark Matter Search Results from the Complete Exposure of the PICO-60 C_3F_8 Bubble Chamber. *Phys. Rev. D*, 100(2):022001, 2019.

[30] S. Adrian-Martinez et al. Limits on Dark Matter Annihilation in the Sun using the ANTARES Neutrino Telescope. *Phys. Lett. B*, 759:69–74, 2016.

[31] E. Aprile et al. First Dark Matter Search with Nuclear Recoils from the XENONnT Experiment. *Phys. Rev. Lett.*, 131(4):041003, 2023.

[32] J. Aalbers et al. First Dark Matter Search Results from the LUX-ZEPLIN (LZ) Experiment. *Phys. Rev. Lett.*, 131(4):041002, 2023.

[33] K. Choi et al. Search for neutrinos from annihilation of captured low-mass dark matter particles in the Sun by Super-Kamiokande. *Phys. Rev. Lett.*, 114(14):141301, 2015.

[34] E. Aprile et al. Light Dark Matter Search with Ionization Signals in XENON1T. *Phys. Rev. Lett.*, 123(25):251801, 2019.

PoS(ICRC2025)502

Full Author List: IceCube Collaboration

R. Abbasi[16], M. Ackermann[63], J. Adams[17], S. K. Agarwalla[39, a], J. A. Aguilar[10], M. Ahlers[21], J.M. Alameddine[22], S. Ali[35], N. M. Amin[43], K. Andeen[41], C. Argüelles[13], Y. Ashida[52], S. Athanasiadou[63], S. N. Axani[43], R. Babu[23], X. Bai[49], J. Baines-Holmes[39], A. Balagopal V.[39, 43], S. W. Barwick[29], S. Bash[26], V. Basu[52], R. Bay[6], J. J. Beatty[19, 20], J. Becker Tjus[9, b], P. Behrens[1], J. Beise[61], C. Bellenghi[26], B. Benkel[63], S. BenZvi[51], D. Berley[18], E. Bernardini[47, c], D. Z. Besson[35], E. Blaufuss[18], L. Bloom[58], S. Blot[63], I. Bodo[39], F. Bontempo[30], J. Y. Book Motzkin[13], C. Boscolo Meneguolo[47, c], S. Böser[40], O. Botner[61], J. Böttcher[1], J. Braun[39], B. Brinson[4], Z. Brisson-Tsavoussis[32], R. T. Burley[2], D. Butterfield[39], M. A. Campana[48], K. Carloni[13], J. Carpio[33, 34], S. Chattopadhyay[39, a], N. Chau[10], Z. Chen[55], D. Chirkin[39], S. Choi[52], B. A. Clark[18], A. Coleman[61], P. Coleman[1], G. H. Collin[14], D. A. Coloma Borja[47], A. Connolly[19, 20], J. M. Conrad[14], R. Corley[52], D. F. Cowen[59, 60], C. De Clercq[11], J. J. DeLaunay[59], D. Delgado[13], T. Delmeulle[10], S. Deng[1], P. Desiati[39], K. D. de Vries[11], G. de Wasseige[36], T. DeYoung[23], J. C. Díaz-Vélez[39], S. DiKerby[23], M. Dittmer[42], A. Domi[25], L. Draper[52], L. Dueser[1], D. Durnford[24], K. Dutta[40], M. A. DuVernois[39], T. Ehrhardt[40], L. Eidenschink[26], A. Eimer[25], P. Eller[26], E. Ellinger[62], D. Elsässer[22], R. Engel[30, 31], H. Erpenbeck[39], W. Esmail[42], S. Eulig[13], J. Evans[18], P. A. Evenson[43], K. L. Fan[18], K. Fang[39], K. Farrag[15], A. R. Fazely[5], A. Fedynitch[57], N. Feigl[8], C. Finley[54], L. Fischer[63], D. Fox[59], A. Franckowiak[9], S. Fukami[63], P. Fürst[1], J. Gallagher[38], E. Ganster[1], A. Garcia[13], M. Garcia[43], G. Garg[39, a], E. Genton[13, 36], L. Gerhardt[7], A. Ghadimi[58], C. Glaser[61], T. Glüsenkamp[61], J. G. Gonzalez[43], S. Goswami[33, 34], A. Granados[23], D. Grant[12], S. J. Gray[18], S. Griffin[39], S. Griswold[51], K. M. Groth[21], D. Guevel[39], C. Günther[1], P. Gutjahr[22], C. Ha[53], C. Haack[25], A. Hallgren[61], L. Halve[1], F. Halzen[39], L. Hamacher[1], M. Ha Minh[26], M. Handt[1], K. Hanson[39], J. Hardin[14], A. A. Harnisch[23], P. Hatch[32], A. Haungs[30], J. Häußler[1], K. Helbing[62], J. Hellrung[9], B. Henke[23], L. Hennig[25], F. Henningsen[12], L. Heuermann[1], R. Hewett[17], N. Heyer[61], S. Hickford[62], A. Hidvegi[54], C. Hill[15], G. C. Hill[2], R. Hmaid[15], K. D. Hoffman[18], D. Hooper[39], S. Hori[39], K. Hoshina[39, d], M. Hostert[13], W. Hou[30], T. Huber[30], K. Hultqvist[54], K. Hymon[22, 57], A. Ishihara[15], W. Iwakiri[15], M. Jacquart[21], S. Jain[39], O. Janik[25], M. Jansson[36], M. Jeong[52], M. Jin[13], N. Kamp[13], D. Kang[30], W. Kang[48], X. Kang[48], A. Kappes[42], L. Kardum[22], T. Karg[63], M. Karl[26], A. Karle[39], A. Katil[24], M. Kauer[39], J. L. Kelley[39], M. Khanal[52], A. Khatee Zathul[39], A. Kheirandish[33, 34], H. Kimku[53], J. Kiryluk[55], C. Klein[25], S. R. Klein[6, 7], Y. Kobayashi[15], A. Kochocki[23], R. Koirala[43], H. Kolanoski[8], T. Kontrimas[26], L. Köpke[40], C. Kopper[25], D. J. Koskinen[21], P. Koundal[43], M. Kowalski[8, 63], T. Kozynets[21], N. Krieger[9], J. Krishnamoorthi[39, a], T. Krishnan[13], K. Kruiswijk[36], E. Krupczak[23], A. Kumar[63], E. Kun[9], N. Kurahashi[48], N. Lad[63], C. Lagunas Gualda[26], L. Lallement Arnaud[10], M. Lamoureux[36], M. J. Larson[18], F. Lauber[62], J. P. Lazar[36], K. Leonard DeHolton[60], A. Leszczyńska[43], J. Liao[4], C. Lin[43], Y. T. Liu[60], M. Liubarska[24], C. Love[48], L. Lu[39], F. Lucarelli[27], W. Luszczak[19, 20], Y. Lyu[6, 7], J. Madsen[39], E. Magnus[11], K. B. M. Mahn[23], Y. Makino[39], E. Manao[26], S. Mancina[47, e], A. Mand[39], I. C. Mariş[10], S. Marka[45], Z. Marka[45], L. Marten[1], I. Martinez-Soler[13], R. Maruyama[44], J. Mauro[36], F. Mayhew[23], F. McNally[37], J. V. Mead[21], K. Meagher[39], S. Mechbal[63], A. Medina[20], M. Meier[15], Y. Merckx[11], L. Merten[9], J. Mitchell[5], L. Molchany[49], T. Montaruli[27], R. W. Moore[24], Y. Morii[15], A. Mosbrugger[25], M. Moulai[39], D. Mousadi[63], E. Moyaux[36], T. Mukherjee[30], R. Naab[63], M. Nakos[39], U. Naumann[62], J. Necker[63], L. Neste[54], M. Neumann[42], H. Niederhausen[23], M. U. Nisa[23], K. Noda[15], A. Noell[1], A. Novikov[43], A. Obertacke Pollmann[15], V. O'Dell[39], A. Olivas[18], R. Orsoe[26], J. Osborn[39], E. O'Sullivan[61], V. Palusova[40], H. Pandya[43], A. Parenti[10], N. Park[32], V. Parrish[23], E. N. Paudel[58], L. Paul[49], C. Pérez de los Heros[61], T. Pernice[63], J. Peterson[39], M. Plum[49], A. Pontén[61], V. Poojyam[58], Y. Popovych[40], M. Prado Rodriguez[39], B. Pries[23], R. Procter-Murphy[18], G. T. Przybylski[7], L. Pyras[52], C. Raab[36], J. Rack-Helleis[40], N. Rad[63], M. Ravn[61], K. Rawlins[3], Z. Rechav[39], A. Rehman[43], I. Reistroffer[49], E. Resconi[26], S. Reusch[63], C. D. Rho[56], W. Rhode[22], L. Ricca[36], B. Riedel[39], A. Rifaie[62], E. J. Roberts[2], S. Robertson[6, 7], M. Rongen[25], A. Rosted[15], C. Rott[52], T. Ruhe[22], L. Ruohan[26], D. Ryckbosch[28], J. Saffer[31], D. Salazar-Gallegos[23], P. Sampathkumar[30], A. Sandrock[62], G. Sanger-Johnson[23], M. Santander[58], S. Sarkar[46], J. Savelberg[1], M. Scarnera[36], P. Schaile[26], M. Schaufel[1], H. Schieler[30], S. Schindler[25], L. Schlickmann[40], B. Schlüter[42], F. Schlüter[10], N. Schmeisser[62], T. Schmidt[18], F. G. Schröder[30, 43], L. Schumacher[25], S. Schwirn[1], S. Sclafani[18], D. Seckel[43], L. Seen[39], M. Seikh[35], S. Seunarine[50], P. A. Sevle Myhr[36], R. Shah[48], S. Shefali[31], N. Shimizu[15], B. Skrzypek[6], R. Snihur[39], J. Soedingrekso[22], A. Søgaard[21], D. Soldin[52], P. Soldin[1], G. Sommani[9], C. Spannfellner[26], G. M. Spiczak[50], C. Spiering[63], J. Stachurska[28], M. Stamatikos[20], T. Stanev[43], T. Stezelberger[7], T. Stürwald[62], T. Stuttard[21], G. W. Sullivan[18], I. Taboada[4], S. Ter-Antonyan[5], A. Terliuk[26], A. Thakuri[49], M. Thiesmeyer[39], W. G. Thompson[13], J. Thwaites[39], S. Tilav[43], K. Tollefson[23], S. Toscano[10], D. Tosi[39], A. Trettin[63], A. K. Upadhyay[39, a], K. Upshaw[5], A. Vaidyanathan[41], N. Valtonen-Mattila[9, 61], J. Valverde[41], J. Vandenbroucke[39], T. van Eeden[63], N. van Eijndhoven[11], L. van Rootselaar[22], J. van Santen[63], F. J. Vara Carbonell[42], F. Varsi[31], M. Venugopal[30], M. Vereecken[36], S. Vergara Carrasco[17], S. Verpoest[43], D. Veske[45], A. Vijai[18], J. Villarreal[14], C. Walck[54], A. Wang[4], E. Warrick[58], C. Weaver[23], P. Weigel[14], A. Weindl[30], J. Weldert[40], A. Y. Wen[13], C. Wendt[39], J. Werthebach[22], M. Weyrauch[30], N. Whitehorn[23], C. H. Wiebusch[1], D. R. Williams[58], L. Witthaus[22], M. Wolf[26], G. Wrede[25], X. W. Xu[5], J. P. Yañez[24], Y. Yao[39], E. Yildizci[39], S. Yoshida[15], R. Young[35], F. Yu[13], S. Yu[52], T. Yuan[39], A. Zegarelli[9], S. Zhang[23], Z. Zhang[55], P. Zhelnin[13], P. Zilberman[39]

[1] III. Physikalisches Institut, RWTH Aachen University, D-52056 Aachen, Germany
[2] Department of Physics, University of Adelaide, Adelaide, 5005, Australia
[3] Dept. of Physics and Astronomy, University of Alaska Anchorage, 3211 Providence Dr., Anchorage, AK 99508, USA
[4] School of Physics and Center for Relativistic Astrophysics, Georgia Institute of Technology, Atlanta, GA 30332, USA
[5] Dept. of Physics, Southern University, Baton Rouge, LA 70813, USA
[6] Dept. of Physics, University of California, Berkeley, CA 94720, USA
[7] Lawrence Berkeley National Laboratory, Berkeley, CA 94720, USA
[8] Institut für Physik, Humboldt-Universität zu Berlin, D-12489 Berlin, Germany
[9] Fakultät für Physik & Astronomie, Ruhr-Universität Bochum, D-44780 Bochum, Germany
[10] Université Libre de Bruxelles, Science Faculty CP230, B-1050 Brussels, Belgium

PoS(ICRC2025)502

[11] Vrije Universiteit Brussel (VUB), Dienst ELEM, B-1050 Brussels, Belgium
[12] Dept. of Physics, Simon Fraser University, Burnaby, BC V5A 1S6, Canada
[13] Department of Physics and Laboratory for Particle Physics and Cosmology, Harvard University, Cambridge, MA 02138, USA
[14] Dept. of Physics, Massachusetts Institute of Technology, Cambridge, MA 02139, USA
[15] Dept. of Physics and The International Center for Hadron Astrophysics, Chiba University, Chiba 263-8522, Japan
[16] Department of Physics, Loyola University Chicago, Chicago, IL 60660, USA
[17] Dept. of Physics and Astronomy, University of Canterbury, Private Bag 4800, Christchurch, New Zealand
[18] Dept. of Physics, University of Maryland, College Park, MD 20742, USA
[19] Dept. of Astronomy, Ohio State University, Columbus, OH 43210, USA
[20] Dept. of Physics and Center for Cosmology and Astro-Particle Physics, Ohio State University, Columbus, OH 43210, USA
[21] Niels Bohr Institute, University of Copenhagen, DK-2100 Copenhagen, Denmark
[22] Dept. of Physics, TU Dortmund University, D-44221 Dortmund, Germany
[23] Dept. of Physics and Astronomy, Michigan State University, East Lansing, MI 48824, USA
[24] Dept. of Physics, University of Alberta, Edmonton, Alberta, T6G 2E1, Canada
[25] Erlangen Centre for Astroparticle Physics, Friedrich-Alexander-Universität Erlangen-Nürnberg, D-91058 Erlangen, Germany
[26] Physik-department, Technische Universität München, D-85748 Garching, Germany
[27] Département de physique nucléaire et corpusculaire, Université de Genève, CH-1211 Genève, Switzerland
[28] Dept. of Physics and Astronomy, University of Gent, B-9000 Gent, Belgium
[29] Dept. of Physics and Astronomy, University of California, Irvine, CA 92697, USA
[30] Karlsruhe Institute of Technology, Institute for Astroparticle Physics, D-76021 Karlsruhe, Germany
[31] Karlsruhe Institute of Technology, Institute of Experimental Particle Physics, D-76021 Karlsruhe, Germany
[32] Dept. of Physics, Engineering Physics, and Astronomy, Queen's University, Kingston, ON K7L 3N6, Canada
[33] Department of Physics & Astronomy, University of Nevada, Las Vegas, NV 89154, USA
[34] Nevada Center for Astrophysics, University of Nevada, Las Vegas, NV 89154, USA
[35] Dept. of Physics and Astronomy, University of Kansas, Lawrence, KS 66045, USA
[36] Centre for Cosmology, Particle Physics and Phenomenology - CP3, Université catholique de Louvain, Louvain-la-Neuve, Belgium
[37] Department of Physics, Mercer University, Macon, GA 31207-0001, USA
[38] Dept. of Astronomy, University of Wisconsin—Madison, Madison, WI 53706, USA
[39] Dept. of Physics and Wisconsin IceCube Particle Astrophysics Center, University of Wisconsin—Madison, Madison, WI 53706, USA
[40] Institute of Physics, University of Mainz, Staudinger Weg 7, D-55099 Mainz, Germany
[41] Department of Physics, Marquette University, Milwaukee, WI 53201, USA
[42] Institut für Kernphysik, Universität Münster, D-48149 Münster, Germany
[43] Bartol Research Institute and Dept. of Physics and Astronomy, University of Delaware, Newark, DE 19716, USA
[44] Dept. of Physics, Yale University, New Haven, CT 06520, USA
[45] Columbia Astrophysics and Nevis Laboratories, Columbia University, New York, NY 10027, USA
[46] Dept. of Physics, University of Oxford, Parks Road, Oxford OX1 3PU, United Kingdom
[47] Dipartimento di Fisica e Astronomia Galileo Galilei, Università Degli Studi di Padova, I-35122 Padova PD, Italy
[48] Dept. of Physics, Drexel University, 3141 Chestnut Street, Philadelphia, PA 19104, USA
[49] Physics Department, South Dakota School of Mines and Technology, Rapid City, SD 57701, USA
[50] Dept. of Physics, University of Wisconsin, River Falls, WI 54022, USA
[51] Dept. of Physics and Astronomy, University of Rochester, Rochester, NY 14627, USA
[52] Department of Physics and Astronomy, University of Utah, Salt Lake City, UT 84112, USA
[53] Dept. of Physics, Chung-Ang University, Seoul 06974, Republic of Korea
[54] Oskar Klein Centre and Dept. of Physics, Stockholm University, SE-10691 Stockholm, Sweden
[55] Dept. of Physics and Astronomy, Stony Brook University, Stony Brook, NY 11794-3800, USA
[56] Dept. of Physics, Sungkyunkwan University, Suwon 16419, Republic of Korea
[57] Institute of Physics, Academia Sinica, Taipei, 11529, Taiwan
[58] Dept. of Physics and Astronomy, University of Alabama, Tuscaloosa, AL 35487, USA
[59] Dept. of Astronomy and Astrophysics, Pennsylvania State University, University Park, PA 16802, USA
[60] Dept. of Physics, Pennsylvania State University, University Park, PA 16802, USA
[61] Dept. of Physics and Astronomy, Uppsala University, Box 516, SE-75120 Uppsala, Sweden
[62] Dept. of Physics, University of Wuppertal, D-42119 Wuppertal, Germany
[63] Deutsches Elektronen-Synchrotron DESY, Platanenallee 6, D-15738 Zeuthen, Germany
[a] also at Institute of Physics, Sachivalaya Marg, Sainik School Post, Bhubaneswar 751005, India
[b] also at Department of Space, Earth and Environment, Chalmers University of Technology, 412 96 Gothenburg, Sweden
[c] also at INFN Padova, I-35131 Padova, Italy
[d] also at Earthquake Research Institute, University of Tokyo, Bunkyo, Tokyo 113-0032, Japan
[e] now at INFN Padova, I-35131 Padova, Italy

PoS(ICRC2025)502

Acknowledgments

The authors gratefully acknowledge the support from the following agencies and institutions: USA – U.S. National Science Foundation-Office of Polar Programs, U.S. National Science Foundation-Physics Division, U.S. National Science Foundation-EPSCoR, U.S. National Science Foundation-Office of Advanced Cyberinfrastructure, Wisconsin Alumni Research Foundation, Center for High Throughput Computing (CHTC) at the University of Wisconsin–Madison, Open Science Grid (OSG), Partnership to Advance Throughput Computing (PATh), Advanced Cyberinfrastructure Coordination Ecosystem: Services & Support (ACCESS), Frontera and Ranch computing project at the Texas Advanced Computing Center, U.S. Department of Energy-National Energy Research Scientific Computing Center, Particle astrophysics research computing center at the University of Maryland, Institute for Cyber-Enabled Research at Michigan State University, Astroparticle physics computational facility at Marquette University, NVIDIA Corporation, and Google Cloud Platform; Belgium – Funds for Scientific Research (FRS-FNRS and FWO), FWO Odysseus and Big Science programmes, and Belgian Federal Science Policy Office (Belspo); Germany – Bundesministerium für Forschung, Technologie und Raumfahrt (BMFTR), Deutsche Forschungsgemeinschaft (DFG), Helmholtz Alliance for Astroparticle Physics (HAP), Initiative and Networking Fund of the Helmholtz Association, Deutsches Elektronen Synchrotron (DESY), and High Performance Computing cluster of the RWTH Aachen; Sweden – Swedish Research Council, Swedish Polar Research Secretariat, Swedish National Infrastructure for Computing (SNIC), and Knut and Alice Wallenberg Foundation; European Union – EGI Advanced Computing for research; Australia – Australian Research Council; Canada – Natural Sciences and Engineering Research Council of Canada, Calcul Québec, Compute Ontario, Canada Foundation for Innovation, WestGrid, and Digital Research Alliance of Canada; Denmark – Villum Fonden, Carlsberg Foundation, and European Commission; New Zealand – Marsden Fund; Japan – Japan Society for Promotion of Science (JSPS) and Institute for Global Prominent Research (IGPR) of Chiba University; Korea – National Research Foundation of Korea (NRF); Switzerland – Swiss National Science Foundation (SNSF).

PoS(ICRC2025)502